

Specific responses of human hippocampal neurons are associated with better memory

Nanthia A. Suthana^{a,b,1}, Neelroop N. Parikshak^a, Arne D. Ekstrom^c, Matias J. Ison^d, Barbara J. Knowlton^e, Susan Y. Bookheimer^{b,e}, and Itzhak Fried^{a,f,1}

^aDepartment of Neurosurgery, David Geffen School of Medicine and Semel Institute For Neuroscience and Human Behavior, University of California, Los Angeles, CA 90095; ^bDepartment of Psychiatry and Biobehavioral Sciences, Semel Institute, University of California, Los Angeles, CA 90095; ^cCenter For Neuroscience and Department of Psychology, University of California, Davis, CA 95616; ^dDepartment of Engineering and Centre for Systems Neuroscience, University of Leicester, Leicester LE1 7RH, United Kingdom; ^eDepartment of Psychology, University of California, Los Angeles, CA 90095; and ^fFunctional Neurosurgery Unit, Tel-Aviv Medical Center and Sackler School of Medicine, Tel-Aviv University, Tel-Aviv 69978, Israel

Edited by Michael E. Goldberg, Columbia University College of Physicians and Surgeons and the New York State Psychiatric Institute, New York, NY, and approved April 10, 2015 (received for review December 7, 2014)

A population of human hippocampal neurons has shown responses to individual concepts (e.g., Jennifer Aniston) that generalize to different instances of the concept. However, recordings from the rodent hippocampus suggest an important function of these neurons is their ability to discriminate overlapping representations, or pattern separate, a process that may facilitate discrimination of similar events for successful memory. In the current study, we explored whether human hippocampal neurons can also demonstrate the ability to discriminate between overlapping representations and whether this selectivity could be directly related to memory performance. We show that among medial temporal lobe (MTL) neurons, certain populations of neurons are selective for a previously studied (target) image in that they show a significant decrease in firing rate to very similar (lure) images. We found that a greater proportion of these neurons can be found in the hippocampus compared with other MTL regions, and that memory for individual items is correlated to the degree of selectivity of hippocampal neurons responsive to those items. Moreover, a greater proportion of hippocampal neurons showed selective firing for target images in good compared with poor performers, with overall memory performance correlated with hippocampal selectivity. In contrast, selectivity in other MTL regions was not associated with memory performance. These findings show that a substantial proportion of human hippocampal neurons encode specific memories that support the discrimination of overlapping representations. These results also provide previously unidentified evidence consistent with a unique role of the human hippocampus in orthogonalization of representations in declarative memory.

hippocampus | memory | selectivity | invariance | discrimination

A cornerstone of memory is the ability to discriminate among similar events (e.g., remembering where one parked his/her car today as opposed to yesterday). To discriminate and retrieve similar memories effectively, it is necessary to maintain separation of their neural representations. While the entire medial temporal lobe (MTL) is crucial for the formation of new declarative memories for facts and events (1, 2), focal hippocampal lesions can lead to selective deficits in recognition memory whereby discrimination of previously learned items from novel similar items is impaired (3, 4). Consistent with these findings, the hippocampus is thought to orthogonalize or separate overlapping information to support memory specificity (5). Results supporting this idea come from human fMRI studies showing that the blood-oxygenated level dependent (BOLD) signal in the combined area of CA3 and dentate gyrus (CA3DG) of the hippocampus differentiates between old (targets) and novel similar (lure) images (6, 7). However, because the hippocampal BOLD response does not always reflect underlying single neuron activity (8), intracranial recordings from single neurons in humans can be more directly informative. For example, single neurons within

the human hippocampus have been found to significantly increase in firing rate to varying photographs of an individual face (e.g., Jennifer Aniston; refs. 9–12), suggesting that hippocampal neurons may participate in concept representations that are not specific to a single stimulus. It is unknown whether a different population of hippocampal neurons exists that are selective for specific stimuli (i.e., a particular photograph of a face) and whether activity in these neurons supports the role of the hippocampus in discrimination of overlapping memory representations.

The current study sought to determine whether the neuronal code reflecting the creation of specific memories could be reflected at the single neuron level in humans. With the rare opportunity to work with patients undergoing clinical evaluation for possible surgical therapy, we were able to record human MTL neurons while subjects were engaged in a hippocampal-dependent memory task requiring the discrimination of studied targets from similar unstudied lures. We hypothesized that firing in a population of hippocampal neurons would reflect memory specificity by firing in a selective manner that discriminates previously learned targets from similar lures. We predicted that firing rate increases that were specific to targets would not generalize to similar lures. Given the suggested role of the hippocampus in pattern separation for memory, we predicted that the specificity of hippocampal firing would be related to the participant's performance on the discrimination task. We further hypothesized that this relationship would be specific to hippocampal neurons, whereas the firing pattern of neurons in other

Significance

Neurons within the human hippocampus have been shown to respond to individual concepts such as varying photographs of a single famous person. However, the relationship between these invariant neuronal responses and hippocampal-dependent memory remains elusive. The current study explores whether the specificity of human hippocampal neuronal responses can be directly related to memory performance. Our results provide a previously unidentified link between human hippocampal single-unit firing patterns and declarative memory performance, ultimately contributing to our understanding of the medial temporal lobe system from single neurons to human behavior.

Author contributions: N.A.S., A.D.E., B.J.K., S.Y.B., and I.F. designed research; N.A.S., A.D.E., and M.J.I. performed research; N.A.S., N.N.P., and M.J.I. analyzed data; and N.A.S., N.N.P., B.J.K., and I.F. wrote the paper.

The authors declare no conflict of interest.

This article is a PNAS Direct Submission.

Freely available online through the PNAS open access option.

¹To whom correspondence may be addressed. Email: nanthia@ucla.edu or ifried@mednet.ucla.edu.

This article contains supporting information online at www.pnas.org/lookup/suppl/doi:10.1073/pnas.1423036112/-DCSupplemental.

medial temporal lobe regions which we assessed, including the entorhinal cortex, parahippocampal cortex, and amygdala, would not relate to performance on a test of discrimination ability in memory.

Results

Neuronal activity was recorded during 40 sessions in 25 subjects (mean age \pm SD = 33.2 ± 10.61) while they studied photographs (target images) of famous people, and rejected similar photographs of the same person (lure images) or photographs of a novel person (foil images) during a recognition memory test (Fig. 1A). For data analysis, subject performance was quantified with a discrimination index score (Fig. 1), which subtracted subjects' false alarm rate to foils (novel unstudied images) from their correct rejection rate to the lures (similar but novel photographs of studied images). The discrimination index, based on a separation bias score (7), was calculated for each session by using $[p(\text{"New"}|\text{Lure}) - p(\text{"New"}|\text{Target})]$ and averaged across sessions for subjects that had two testing sessions. A bias score of 1 is the maximal possible score indicating high performance on the memory task. All subjects completed the recognition task [Fig. 2; LP group (12 subjects; $n = 20$ sessions)] average percent correct = 73.4%, range = (65.1–88.7); HP group (13 subjects, $n = 20$ sessions) average percent correct = 95.6%, range = (94.4–99.1). The rate of incorrectly recognizing a lure item as a target (false alarm) slightly decreased as lures became less similar to targets (Fig. S1; Lure 1 = most similar, Lure 3 = least similar). The median of the discrimination index scores across all subjects was used to split subjects into a high performance (HP; greater than the median) and low performance (LP; lower than the median) group.

During the discrimination task, neural activity was simultaneously recorded by intracranial electrodes, and the location of each electrode was localized to hippocampal subregions by using a high-resolution 3T hippocampal scan (0.4×0.4 mm in-plane) and visualized on a simplified unfolded 2D map of MTL regions (Fig. S2; refs. 13 and 14). Electrode locations were also confirmed on the 3D image based on visual MRI landmarks from known histological atlases. For localization of all electrodes, see Table S1. For demographic information of participants, including age, sex, and neuropsychological scores, see Table S2. There were no significant differences between the HP and LP group in age and on nonmnemonic neuropsychological test scores. There were, however, significant differences between the HP and LP groups on tests of long-term memory as measured by the logical memory

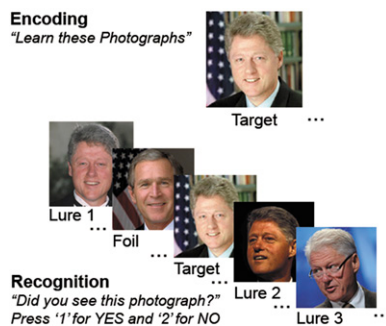


Fig. 1. Subjects learned (encoding) and recognized (recognition) photographs of famous faces. During the encoding block, subjects saw 10 photographs of 10 famous individuals in random order and were instructed to learn the photographs. During the recognition block, subjects saw previously learned (target) photographs and novel (lure and foil) photographs and were asked whether they had seen the photograph before by pressing one of two buttons. (Top) Image courtesy of Bob McNeeley (The White House). (Bottom, Left to Right) Images courtesy of ©ImageCollect.com/Alpha-Globe Photos, Inc.; US Department of Defense and Eric Draper; Bob McNeeley (The White House); and ©ImageCollect.com photographers James Colburn/ipo/Globe Photos, Inc. and acepixs.

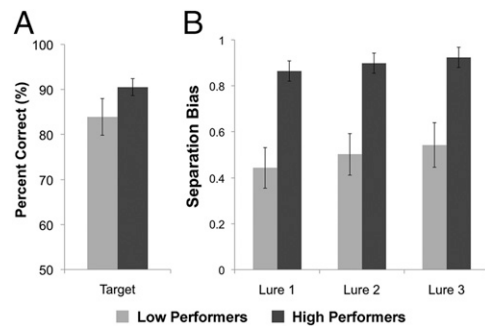


Fig. 2. (A) Shown is percentage correct for recognition of the target image averaged across 40 sessions from 25 patients ($n = 40$) split into low and high performers. (B) Shown is the memory performance for lure images as measured by the discrimination index score ($p(\text{"New"}|\text{Lure}) - p(\text{"New"}|\text{Target})$). A discrimination index score of 1 would be the maximal possible score, indicating high performance on the memory task. Lure 1 = most similar and lure 3 = least similar to the target photograph.

portion of the Wechsler Memory Scale (HP > LP, $z = 3.2$, $P = 0.001$) and long-delay free-recall portion of the California Verbal Learning Test (HP > LP, $z = 2.6$, $P = 0.009$).

To optimize the number of units responsive to a target (target-responsive units) during the experimental session, subjects completed a screening session before the experimental session. Unit responsiveness during the screening session identified "famous people" to use for the discrimination task. Importantly, only novel photographs of each famous person were used for the discrimination task. For each famous person, four additional novel photographs were used for the memory retrieval task: three similar lure images of the same person and one foil image of a different person (see further details of paradigm in *Methods*). During the experimental sessions, recordings were taken from 1,176 individual units [Table S3; 586 in the LP group Table S4; [hippocampus: 129, entorhinal cortex (ERC): 133, parahippocampal cortex (PHC): 109, amygdala: 215], 590 in the HP group (Table S5; hippocampus: 156, ERC: 119, PHC: 117, amygdala: 198)]. Significant responses to an image were quantified by using previously published methods (*Methods*). In total, approximately one-third of MTL units recorded (417/1,176, 35.6%) showed significantly altered activity during the recognition of the original target image; significantly active neurons were quantified by using previously published methods (see *Methods* section for details). Of these 417 target-responsive units, 110 were localized to the hippocampus; 62 of these 110 were in the CA3DG region (LP: 30 units, HP: 32 units), and 37 of these 110 were in the subiculum (LP: 15 units, HP: 32 units); for 11 units, we were unable to perform localization to a specific hippocampal subregion because of the unavailability of a high-resolution MRI scan. Of the remaining target-responsive units, 91 units were localized to the ERC (LP: 38 units, HP: 53 units), 105 units were localized to the PHC (LP: 41 units, HP: 64 units), and 111 units were localized to the amygdala (LP: 61 units, HP: 50 units).

There were differences between the HP and LP groups in terms of the selectivity of hippocampal target-responsive units. In the HP group compared with the LP group, a greater proportion of target-responsive units in CA3DG and subiculum responded only to the target [target-selective units (Fig. 2A; CA3DG, $\chi^2 = 7.07$; $P = 0.008$; subiculum, $\chi^2 = 4.70$; $P = 0.03$)]. In the ERC, PHC, and the amygdala, the proportion of target-selective units was similar for the HP and LP group (ERC, $\chi^2 = 0.058$; $P = 0.81$; PHC, $\chi^2 = 0.04$; $P = 0.84$; amygdala, $\chi^2 = 0.05$, $P = 0.83$). These results indicate that in high performers, neurons in the hippocampus are more likely to differentiate between studied items and very similar items. In contrast, the proportions of neurons in the ERC, PHC, and amygdala that respond selectively were similar in high and low performers. Fig. 3 shows example neuronal responses

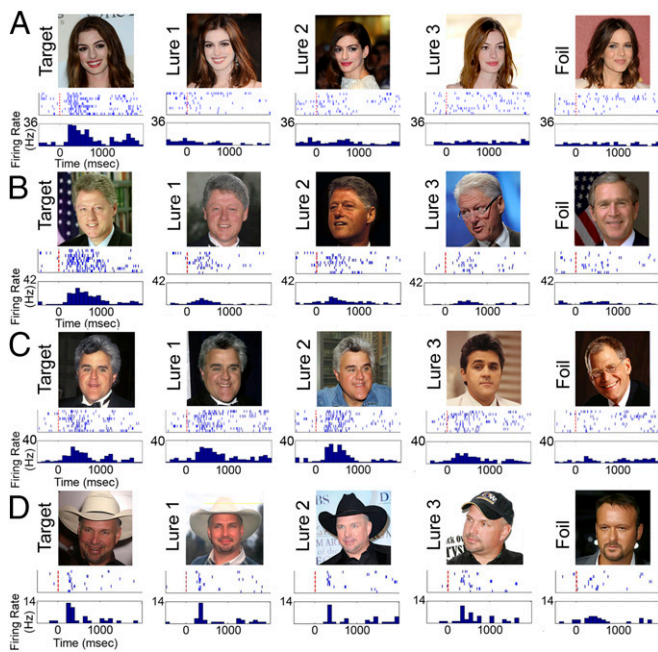


Fig. 3. Example single-unit responses. An example of a target-selective unit in the CA3 and dentate gyrus (CA3DG) (A) and subiculum (B) in a high performer, which significantly increases in firing rate (Hertz) to the target image much more so than to the lure and foil images during retrieval. (C and D) Shown is an example of a target-responsive unit in CA3DG in a low performer, which significantly increases in firing rate similarly to both the target and lure image. Images courtesy of (A, Left to Right) ©ImageCollect.com photographers Ken Babolcsay-Ipol/Globe Photo, StarMaxWorldwide, Acepixs, Roger Harvey-Globe Photos, Byron Purvis/AdMedia; (B, Left to Right) Bob McNeely (The White House); ©ImageCollect.com photographers Alpha-Globe Photos Inc., James Colburn/Ipol/Globe Photos Inc., and acepixs; US Department of Defense and Eric Draper; (C, Left to Right) ©ImageCollect.com photographers Jonathan Alcorn/ZUMA Press, Paul Skipper/glob Ephotos Inc., Ken Babolcsay/Ipol/Globe Photos Inc., Donald Sanders-Globe Photos Inc., Christopher Little/cbs; (D, Left to Right) ©ImageCollect.com photographers Rick Mackler Rangefinder-Globe Photos Inc., StarMaxWorldwide, s_bukley, Nina Prommer-Globe Photos Inc., Clinton H. Wallace/Ipol/Globe Photos Inc.

to target, lure, and foil images in hippocampal CA3DG and subiculum regions of HP and LP groups; target-selective neurons significantly increase in firing rate compared with baseline to the target image only and not significantly to similar lure images (Fig. 3A and B). Overall firing rate and the percentage of target responsive neurons were similar in both groups (HP > LP group: $z = 0.77$, $P = 0.44$) as was the proportion of target-responsive neurons between the two groups (HP vs. LP group: CA3DG: $\chi^2 = 2.27$, $P = 0.13$, subiculum: $\chi^2 = 0.13$, $P = 0.72$). For average firing rates of target responsive neurons across both the HP and LP groups, see Fig. S3. To determine any differences in firing rate during encoding versus retrieval of the target image and to investigate whether repetition suppression effects across trials induces the firing rate changes, we calculated the normalized spike counts for each of the nine target trials across the task during encoding and retrieval of the target image (Fig. S4). We did not find a significant interaction between task condition (encoding vs. retrieval) and trial number on normalized spike counts of target-responsive neurons in the amygdala [$F_{(8,1980)} = 1.467$, $P =$ not significant (n.s.)], CA3DG [$F_{(8,1098)} = 1.07$, $P =$ n.s.], subiculum [$F_{(8,648)} = 1.396$, $P =$ n.s.], or entorhinal cortex [$F_{(8,1620)} = 1.632$, $P =$ n.s.]. We did see a significant interaction between condition and trial number on spike counts of target-responsive neurons within the PHC [$F_{(8,1872)} = 3.84$, $P < 0.05$] and

a main effect of trial ($P < 0.05$) but no effect of condition (encoding vs. retrieval, $P =$ n.s.).

To further investigate how subjects' memory performance related to the pattern of neural firing in different MTL regions, we calculated the difference in average firing rate from baseline across all target-responsive units in each region. We then determined whether memory performance across the entire set of subjects (HP and LP) would correlate with the percentage reduction in averaged hippocampal firing rate from the target to lure 1 image. Remarkably, only in the hippocampus (CA3DG and subiculum) did the percentage reduction of the average firing rate from the target to the lure 1 image significantly correlate with memory performance across all subjects (Fig. 4B; Hippocampus: $\rho = 0.49$, $P = 0.01$; CA3DG: $\rho = 0.65$, $P = 0.029$) and within the HP ($\rho = 0.80$, $P < 0.001$) and LP ($\rho = 0.64$, $P = 0.04$) groups. We found no similar significant effect across the group within the ERC and PHC combined ($\rho = 0.09$, $P = 0.65$) or amygdala ($\rho = 0.27$, $P = 0.19$). We also computed correlation coefficient values between behavioral discrimination indices and target-lure neuronal firing rate changes for specific learned target items within each subject and found them across the group to be significantly above zero within the hippocampus (average $\rho = 0.32$; t -stat = 2.36, $P < 0.05$; Fig. S5A) but not the parahippocampal gyrus (average $\rho = 0.05$; t -stat = 0.53, $P > 0.05$; Fig. S5B). Example individual subject hippocampal scatterplots showing discrimination indices for specific face stimuli and the associated target-lure firing rate changes are shown in Fig. S6. Overall, these data suggest a specific role for the hippocampus in differentiating similar inputs, and that the degree to which the hippocampal neuron firing rates discriminate these images reflects performance on a memory task requiring discrimination.

Discussion

Altogether, we found a greater proportion of target-selective units in the hippocampi of subjects who were able to effectively discriminate old from similar new items in memory compared with those who performed poorly on the test. The magnitude of decrease in the firing rate from targets versus very similar lures correlated with memory performance across the group, and this correlation was specific to the hippocampus. In contrast, firing rate changes from the target to similar lures in ERC, PHC, and amygdala neurons were not related to memory performance.

Collectively, these data show that for individual neurons in the human hippocampus, firing-rate selectivity is associated with a better performance on a task requiring mnemonic discrimination. In addition to encoding specific events, the hippocampus is thought to play a role in generalization and maintenance of flexible relationships between events (15, 16). We have also previously described MTL neural responses that reflect this kind of generalization, whereby single neurons are highly selective (e.g., respond to a particular famous person) but show a high degree of invariance (e.g., respond to multiple different images of the same person; refs. 9–12). In the present study, participants performed a task in which they were required to learn specific photographs and discriminate these from similar lures, and thus, forming highly specific memory representations was key to successful performance. Although we did not investigate whether the cells in the current study were invariant to the same degree as those reported (9) (only a limited number of lures were presented in this task), we note that the presence of such cells in the hippocampus is not inconsistent with the presence of invariant cells in the MTL. One possibility is that different cells of the MTL support stimulus discrimination and stimulus invariance and their relative frequency may differ across regions. Another possibility is that the same cells are involved in both processes, and the specific task demands increase the likelihood that cells will exhibit discriminative properties. Indeed, an important difference from our previous work (9) is that we used a memory test in which subjects

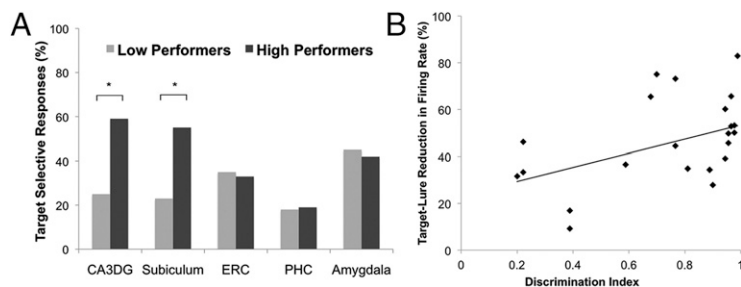


Fig. 4. (A) Shown is the percentage of target-responsive units that significantly increased in firing rate to the target image only (target-selective) and not to lure or foil images. We found more target-selective units within the hippocampus [CA3, and dentate gyrus (CA3DG) and subiculum] in high compared with low performers. No significant differences were found in the proportion of target-selective units in high compared with low performers in the ERC, PHC, or amygdala. (B) Shown is the significant correlation between memory performance (discrimination index score) and the percentage reduction in average firing rate from the target to the most similar lure (Lure 1) in the hippocampus (combined CA3DG and subiculum). Each data point reflects the firing rate reduction from target to lure 1 averaged across all target responsive units within a given subject.

were required to form very specific memory representations to perform well. It is thus possible that top-down influences of task instructions change the firing patterns in the hippocampus. Under these circumstances, modulation of hippocampal activity by projections from other areas may confer additional selectivity and hippocampal neurons may fire in a more restricted manner to specific memorized stimuli (e.g., particular photograph of a famous individual) compared with other MTL regions. In support of the second scenario, of the cells that exhibited invariance during the screening and encoding phases of the experiment, the majority of target-responsive neurons in all MTL regions in this study showed reduced firing for lure photographs of the same individual during the recognition memory task (Fig. S3). In neurons in the hippocampi of high performers, the reduction in firing was particularly pronounced, even for lure photographs that were very similar to the target. In the parahippocampal gyrus, firing rate in target responsive neurons was characterized by a decreasing linear trend as a function of similarity to the target ($F = 4.87$, $P = 0.02$). Interestingly, the pattern of firing in the hippocampus and surrounding parahippocampal gyrus corresponds to the predictions of dual process theories of recognition (17); with firing in the hippocampus consistent with a thresholded recollection response, decreasing sharply and similarly for all nontargets, whereas firing in the parahippocampal gyrus shows a pattern consistent with a familiarity process whereby firing decreases in a graded fashion according to similarity. This study provides unique human neuronal data supporting the idea that the hippocampus and surrounding cortex support different processes in recognition memory (18).

We note that one concern with our comparison of HP and LP epilepsy patients is that general hippocampal pathology could be contributing to the memory impairment and low level of selectivity of responsive neurons in LP groups, rather than the low selectivity being specifically related to memory performance. However, the correlation between memory for specific items and the selectivity of corresponding responsive individual hippocampal neurons demonstrates a relationship between neuronal firing and memory that does not depend on the distinction between the HP and LP groups. Second, even within the HP group, subjects who have relatively normal memory as assessed by neuropsychological testing show a significant correlation between the selectivity of neuronal firing and performance. Third, although hippocampal neurons in the LP group showed less selectivity, it was not the case that hippocampal neural activity appeared generally different from activity in the HP group. Overall firing rate and the percentage of target responsive neurons were similar in both groups as was the proportion of target-responsive neurons between the two groups. Thus, while the presence of epilepsy may have impacted hippocampal function and led to poorer memory in some of the subjects, we believe that overall, the data demonstrate that the selectivity of neuronal firing is reflective of mnemonic processing in the hippocampus. Differences between low and high performers were only apparent when comparing the proportion of significant hippocampal responses to the target versus close lure images. Additionally, there were no differences in the proportion

of target-selective neurons within ERC, PHC, or amygdala regions between low and high performers, thus further supporting the results that memory performance is related specifically to the selectivity of hippocampal neurons to the target images. The results here are the first to our knowledge to demonstrate a correlation between the selective behavior of individual hippocampal neurons and human memory performance.

In the present study, we sampled neurons in both the CA3/dentate gyrus region and the subiculum. Sampling of target responsive neurons in the CA1 was limited (4 of 16 total recorded; Table S3) and, thus, we were unable to assess its firing pattern compared with other hippocampal subregions. Single neuron studies in rodents suggest there are subregional differences in specific firing patterns among hippocampal neurons (19–22). For example, place cells in the dentate gyrus and CA3 often show greater sensitivity to changes in context than those in CA1, at least in some instances (21, 22). Animal studies and computational models suggest dentate gyrus can be biased toward pattern separation-like properties, whereas CA1 can be biased toward pattern completion-like properties (21, 22). Although our analysis limited to the CA3DG region yielded a significant correlation between neuronal selectivity and subsequent memory of specific items, further investigation is required to understand the subtle subregional differences within hippocampal circuit and the contributions of separation vs. completion processes in human memory.

Our current study provides human neuronal evidence for the role of the hippocampus in human memory, suggesting that the formation of individual memory representations is expressed in differential firing of hippocampal neurons and that discriminant firing of these cells is directly related to declarative memory performance in humans. These results can be used to inform circuit-level models of the role of the hippocampus in the encoding and retrieval of distinct episodic memories.

Methods

Subjects. Participants were 25 patients (24 right-handed, 12 female, 20–53 y old, mean age 33.2) with pharmacologically resistant epilepsy implanted with intracranial depth electrodes for 7–14 d to determine epileptogenic zone for possible surgical resection. Electrode placements were determined based on clinical criteria. Subjects provided informed consent and all experimental sessions lasted ~30 min and conformed to the Medical Institutional Review Board at the University of California, Los Angeles (UCLA). Some subjects completed two experimental sessions where completely different sets of photographs were used; multiple sessions were separated by at least 24 h. From 25 subjects there were 40 sessions in total that were completed. For demographic information of high and low performance groups, including age, sex, and neuropsychological scores, see Table S2.

Neuropsychological test scores were determined for subjects including tests of memory and executive function. Specifically, for each subject, Verbal intelligence quotient (IQ) and digit span (i.e., attention) were calculated with the use of the Wechsler Adult Intelligence Scale (23), verbal memory by means of the logical memory portion of the Wechsler Memory Scale (WMS; ref. 24), the long-delay free-recall portion of the California Verbal Learning Test (CVLT; ref. 25), visual memory with the use of the 30-s delayed version of the Rey–Osterrieth Complex Figure Test (26), and executive function by means of the Trail Making Test, Part B (27). A 2×5 ANOVA was used to determine significant differences between low and high performance

groups on neuropsychological test scores. Post hoc Mann–Whitney u tests (Bonferroni corrected at the $P < 0.05$ level) were used to compare neuropsychological test scores between low and high performers.

Screening Session. Before the experimental session, subjects were presented 100 images on a laptop computer in random order six times each for duration of 1 s. The interstimulus interval (ISI) was randomized with a minimum equal to 1.5 s. Subjects responded by making human/nonhuman judgments using two assigned key presses. The data from this screening session was recorded at a sampling rate of 30 kHz on a 128-channel Neuroport (Blackrock Microsystems) or 64-channel Neuralynx recording system and then quickly processed and analyzed offline by using a clustering algorithm *wave_clus* (28) that allows for spike detection and sorting. Significant responses to photographs (stimuli) were calculated by using previous methods (28) where the median number of spikes across the six trials during 300- to 800-ms poststimulus onsets was calculated. The baseline response was determined the same way from 300- to 800-ms prestimulus onsets. A unit was then determined responsive to a particular photograph if the median activity was larger than the average baseline + 5 SDs and the median number of spikes was at least 2.

Experimental Paradigm. From the screening session data and previously published results, units within the MTL responded to various photographs of a given individual (9); these MTL units were indicated as selective units. Based on which famous faces elicited selective units during the screening session, photographs of 10 famous people were then selected for the experimental memory paradigm. None of the photographs from the screening session were used in the experimental session; New photographs of the same individuals were used. Past data shows that with repetitions of the same image, there are small decreases in firing rate, but only of approximately 15% in hippocampal and entorhinal regions and no decrease in the parahippocampal cortex (29). Alternatively, another study has found a subset of neurons that increase in firing rate to repeated stimuli in addition to neurons that decrease in firing rate to repeated stimuli (30). In our dataset, we saw minimal decreases in spiking across trials but no significant differences between encoding and retrieval conditions (Fig. S4). Our paradigm differs from previous repetition suppression findings (29) in that we used an overt memory task where instructions to the participant were clearly different and we limited our firing rate analysis to 300–800 ms after stimulus onset. Also, by using novel photographs during the experimental session, we avoided issues of substantial decreases in firing rate due to repetition suppression effects. During the experimental session, subjects were instructed to learn 10 photographs, which were presented on a laptop screen in a blocked design with three alternating blocks of encoding and retrieval. Each photograph was presented three times in each block (nine total trials) for a duration of 2 s with a jittered intertrial interval of at least 1.5 s. Presentation order was randomized in all blocks. Retrieval blocks consisted of target (studied) photographs, lures (unstudied same face), and foil (unstudied new face) photographs. For every target photograph, three lures and one foil photograph were presented. Subjects were instructed to press one of two buttons if the photograph was old (target) or new (unstudied). Thus, there were a total of 90 encoding trials and 450 retrieval trials (30 encoding and 150 retrieval stimuli per block). Each stimulus was presented nine times total over the course of the experiment. Stimuli were presented, and behavioral responses were recorded by using pyEPL.

Lure Order Determination. For analysis, the order of lures based on similarity to the target image was determined by an independent pool of participants ($n = 24$) who were instructed to place lures in order of decreasing similarity to the target image. In addition, subjects rated photographs after all experimental sessions were completed. Overall neuronal results were not significantly different when using same subjects' or independent subjects' ratings. For main results shown, ratings from the independent pool of participants were used. As expected, the rate of incorrectly recognizing a lure item as a target (false alarm) slightly decreased as lures became less similar to targets (Lure 1 = most similar, Foil = least similar; Fig. S1).

Electrode Recordings. Electrode placement was determined by clinical criteria depending on the suspected seizure focus in each subject. Electrodes contained nine 40- μ m platinum-iridium microwires. Electrophysiological data from the sessions were recorded and filtered between 0.6 and 6 kHz by using a 64-channel Neuralynx recording system sampled at 28 kHz or a 128-channel Neuroport recording system sampled at 30 kHz. For further details on single-unit recording methods used here, see refs. 28, 31, and 32.

Electrode Localization. Before implantation with depth electrodes, subjects were scanned with a Siemens Allegra head-only 3 Tesla magnetic resonance

imaging (MRI) scanner at the UCLA Ronald Reagan Medical Center at the University of California, Los Angeles. Electrodes were localized to hippocampal subregions for nearly all subjects (22 of 25) who underwent a high-resolution 3 Tesla hippocampal scan. Three of the subjects were unable to receive the high-resolution MRI scan because of the presence of metallic implants. High in-plane resolution structural images with a matrix size of 512×512 [spin echo, repetition time (TR) = 5,200 ms, echo time (TE) = 105 ms, 19 slices, contiguous; voxel size: $0.391 \times 0.391 \times 3$ mm] were acquired in the oblique coronal plane perpendicular to the long axis of the hippocampus. The coronal plane was chosen because the structures are relatively homogeneous along the long axis but differ in-plane; thus, we maximize in-plane resolution. Subjects also had a 3-T whole brain T1 weighted MPRAGE GRE scan (TR = 1,800 ms, TE = 2.93 s, voxel size = $0.9 \times 0.9 \times 0.8$ mm) as part of depth-placement planning. Subjects were then implanted with depth electrodes for surgical monitoring. Following implantation with depth electrodes, subjects received a Spiral CT scan (1-s rotation, high-quality mode, helical pitch 1.5, 1-mm slice collimation, and a 0.5-mm reconstruction interval to localize electrodes).

Registering the CT to a whole brain MPRAGE scan in each individual subject was used to localize amygdala electrodes. To localize electrodes to medial temporal subregions, CTs were registered to the high-resolution MRI and to the whole-brain MRI by using a three-way registration in BrainLab stereotactic and localization software (www.brainlab.com; refs. 33 and 34). High-resolution structural scans were then computationally unfolded and flattened from three dimensions to two dimensions, producing flattened maps oriented from bottom to top (posterior to anterior) along the long axis of the hippocampus (Fig. S2C). To create the flat maps, the 3D gray matter of MTL subregions was created (Fig. S2B) using mrGray segmentation software (33). The gray matter was then computationally unfolded using mrUnfold software (mrGray and mrUnfold download: white.stanford.edu/~brian/mri/segmentUnfold.htm; ref. 35), yielding a final voxel size of $0.391 \times 0.391 \times 0.429$ mm (Fig. S2C). The position of the various CA fields, subiculum (sub), entorhinal cortex (ERC), perirhinal cortex (PRC), PHC, and fusiform gyrus on the unfolded map were found by mapping pixels from points demarcated in the structural images based on known atlases (36, 37). See ref. 13 for further details. Because electrophysiological results, including firing rate changes and correlations results, were not significantly different between ERC and PHC regions, we grouped them into a combined encompassing region labeled parahippocampal gyrus (PHG). With our current human imaging methods, the dentate gyrus is not distinguishable from adjacent CA fields and, therefore, grouped in an encompassing region labeled CA3DG (but see ref. 38). The hippocampus is small in structure and variable across subjects, and these methods are unable to reach the resolution necessary to visualize cell histology to determine exact subregional boundaries. However, we deal with this challenge by demarcating each individual subject's boundary locations by using atlases by Amaral and Insausti (36), and Duvernoy (37), which identify landmarks on the MR images by using postmortem histological images.

Electrophysiological Analysis. Data from the experimental session was analyzed offline. Spikes were detected and sorted by using the *wave_clus* program, which uses amplitude thresholding and the wavelet transform to apply superparamagnetic clustering. Furthermore, multiunits and single units were classified based on (i) spike shape and variance; (ii) presence of a refractory period (less than 1% spikes with less than 3 ms ISI); (iii) the ratio between the spike peak value and the noise level; and (iv) the ISI distribution of each cluster. For more information, see ref. 30. When limiting analyses to single units, results were not significantly changed. Therefore, results presented include data from both multiunits and single-units. For the number of recorded single units and multiunits, see Table S3. A previous study on a similar dataset has shown no effect of epileptogenic zone on single-unit firing rate properties (39).

To ensure that neuronal responses were not the results of seizure activity, results were compared after exclusion of data from seizure foci [seven electrode sites, 166/1,176 total neurons excluded (hippocampus: 26/285, ERC: 35/252, PHC: 45/226, amygdala: 60/413)]. Seizure foci were determined by a clinical neurology team and all statistical analysis of neuronal firing rate was determined with and without data from seizure foci excluded. We found no changes in our overall results including the χ^2 analysis (with seizure foci excluded, CA3DG: $\chi^2 = 5.69$; $P < 0.001$; subiculum: $\chi^2 = 4.79$; $P < 0.05$) or our correlation analysis (with neurons from seizure foci excluded, hippocampus: $\rho = 0.59$, $P = 0.03$; PHG: $\rho = 0.08$, $P = 0.83$, amygdala: $\rho = 0.22$, $P = 0.34$) and, therefore, present results calculated with all of the data included.

To determine the relationship between neuronal firing and memory specificity for individual items, we calculated a discrimination index score for each of the 10 famous faces shown to each participant by using the nine trials (three repetitions within each of the three blocks of retrieval) for each of

the 10 images. Thus, for each of the 10 faces there was a calculated discrimination index score with 1 being the maximum value if all nine targets were correctly recognized and all nine of the closest lure (i.e., lure 1) images were correctly rejected for that particular face. Then for target-responsive units, the percent change in firing rate was calculated from the average firing rates across nine trials for the target and closest lure. For participants with at least three statistically significant responses to any target image within a given region (i.e., hippocampal or parahippocampal gyrus), we then calculated a correlation coefficient value between the discrimination indices and the target-lure neuronal firing rate changes. For example, subject values for which such correlation coefficients were calculated (Fig. S6). A one-sample *t* test was then used to determine whether rho values across participants were significantly above zero separately for the hippocampus and parahippocampal gyrus.

For repetition suppression analysis, we calculated the mean normalized number of spikes across repeated trial for encoding and retrieval separately. Specifically, for the 417 MTL target-responsive units during retrieval, we calculated for encoding and, for retrieval, the number of spikes for each trial normalized by dividing by the maximum number of spikes across trials. Note that the average normalized number of spikes does not reach a value of 1 because the maximum number of spikes can occur during different trials across target responses. For further details on method, see ref. 29.

Statistical Analysis. For the experimental session data, units were considered to have a selective response to the target if they exhibited significant increases in firing rate (Hz) compared with baseline by using a nonparametric Mann–Whitney *u* test ($P < 0.05$); poststimulus vs. prestimulus baseline firing rate was compared in the analysis. For units that were thus determined to be responsive to a target image (i.e., target-responsive), we performed nonparametric tests on the same unit's firing rate response to lure 1, lure 2, lure 3, and the foil. If this statistical test yielded significance to any of the latter images (i.e., lures 1–3 or foil), then the unit was categorized as a target-responsive but not target-selective. Only if none of the statistical tests were significant to lures 1–3 or foil was the unit

categorized as target-selective. For each region, the overall change in average firing rate was calculated for the poststimulus interval (300–800 ms) minus the prestimulus interval (–500 to 0 ms). These temporal windows were chosen based on results from several studies recording single neurons from the human MTL (for review see ref. 40). We also completed our analyses with poststimulus temporal windows of 200–700 and 400–900 ms to explore early or late responses. However, these temporal windows did not change our overall results. Correlation analyses were done by calculating the Spearman rank coefficient ($P < 0.05$) between percent reduction in hippocampal, ERC, or PHC average firing rate from target to lure 1 and subjects' average discrimination index score for lure 1. We chose the Spearman rank correlation coefficient, rather than the Pearson-rho correlation because we did not expect a linear correlation between the variables. To determine significant differences in firing rates, within each region (CA3DG, subiculum, PHG, and amygdala), we completed one-way analysis of variance (ANOVA) with five conditions (target, lures 1–3, and foil) with up to 5,000 permutations performed for each test (fewer were done when the *P* value already failed significance at the 0.05 level for 5,000 permutations) on the averaged firing rate ratios, which were calculated by dividing poststimulus by prestimulus firing rates from each target-responsive unit. For repetition suppression analysis, we completed a 2 (encoding vs. retrieval condition) \times 9 (trials 1–9) ANOVA was conducted on normalized spike counts with post hoc paired sample *t* test comparisons (Bonferroni corrected) between conditions if ANOVA showed a significant interaction.

ACKNOWLEDGMENTS. We thank Florian Mormann, Rodrigo Quain Quiroga, and Moran Cerf for advice and technical assistance; Eric Behnke, Deena Pourshaban, Sakshi Aggarwal, Vanessa Isiaka, Brooke Salaz, and Mariana Holliday for general assistance; and all of the participants who volunteered for this study. This work was supported by National Institute of Mental Health Grants 5T32 MH015795 and F32 NS050067-03, the National Institute of Neurological Disorders and Stroke (NS033221), and by the National Institute on Drug Abuse 5T90DA022768-02.

- Squire LR, Stark CE, Clark RE (2004) The medial temporal lobe. *Annu Rev Neurosci* 27:279–306.
- Scoville WB, Milner B (1957) Loss of recent memory after bilateral hippocampal lesions. *J Neurol Neurosurg Psychiatry* 20(1):11–21.
- Hopkins RO, Kesner RP, Goldstein M (1995) Memory for novel and familiar spatial and linguistic temporal distance information in hypoxic subjects. *J Int Neuropsychol Soc* 1(5):454–468.
- Holdstock JS, et al. (2002) Under what conditions is recognition spared relative to recall after selective hippocampal damage in humans? *Hippocampus* 12(3):341–351.
- Yassa MA, Stark CE (2011) Pattern separation in the hippocampus. *Trends Neurosci* 34(10):515–525.
- Bakker A, Kirwan CB, Miller M, Stark CE (2008) Pattern separation in the human hippocampal CA3 and dentate gyrus. *Science* 319(5870):1640–1642.
- Yassa MA, et al. (2010) High-resolution structural and functional MRI of hippocampal CA3 and dentate gyrus in patients with amnesic Mild Cognitive Impairment. *Neuroimage* 51(3):1242–1252.
- Ekstrom A (2010) How and when the fMRI BOLD signal relates to underlying neural activity: The danger in dissociation. *Brain Res Brain Res Rev* 62(2):233–244.
- Quiroga RQ, Reddy L, Kreiman G, Koch C, Fried I (2005) Invariant visual representation by single neurons in the human brain. *Nature* 435(7045):1102–1107.
- Waydo S, Kraskov A, Quiroga RQ, Fried I, Koch C (2006) Sparse representation in the human medial temporal lobe. *J Neurosci* 26(40):10232–10234.
- Quiroga RQ, Reddy L, Koch C, Fried I (2007) Decoding visual inputs from multiple neurons in the human temporal lobe. *J Neurophysiol* 98(4):1997–2007.
- Mormann F, et al. (2008) Latency and selectivity of single neurons indicate hierarchical processing in the human medial temporal lobe. *J Neurosci* 28(36):8865–8872.
- Ekstrom A, et al. (2008) High-resolution depth electrode localization and imaging in patients with pharmacologically intractable epilepsy. *J Neurosurg* 108(4):812–815.
- Zeineh MM, Engel SA, Thompson PM, Bookheimer SY (2001) Unfolding the human hippocampus with high resolution structural and functional MRI. *Anat Rec* 265(2):111–120.
- Eichenbaum H (1999) The hippocampus and mechanisms of declarative memory. *Behav Brain Res* 103(2):123–133.
- Kumaran D, McClelland JL (2012) Generalization through the recurrent interaction of episodic memories: A model of the hippocampal system. *Psychol Rev* 119(3):573–616.
- Yonelinas AP (1994) Receiver-operating characteristics in recognition memory: Evidence for a dual-process model. *J Exp Psychol Learn Mem Cogn* 20(6):1341–1354.
- Eichenbaum H, Yonelinas AP, Ranganath C (2007) The medial temporal lobe and recognition memory. *Annu Rev Neurosci* 30:123–152.
- Leutgeb JK, Leutgeb S, Moser MB, Moser EI (2007) Pattern separation in the dentate gyrus and CA3 of the hippocampus. *Science* 315(5814):961–966.
- Lee I, Yoganarasimha D, Rao G, Knierim JJ (2004) Comparison of population coherence of place cells in hippocampal subfields CA1 and CA3. *Nature* 430(6998):456–459.
- Guzowski JF, Knierim JJ, Moser EI (2004) Ensemble dynamics of hippocampal regions CA3 and CA1. *Neuron* 44(4):581–584.
- Leutgeb S, Leutgeb JK, Treves A, Moser MB, Moser EI (2004) Distinct ensemble codes in hippocampal areas CA3 and CA1. *Science* 305(5688):1295–1298.
- Wechsler D (1997) *Wechsler Adult Intelligence Scale* (Psychological Corp, San Antonio, TX), 3rd Ed.
- Wechsler D (2005) *Wechsler Memory Scale* (Psychological Corp/Harcourt Brace Jovanovich, New York), 4th Ed.
- Delis DC, Kramer JH, Kaplan E, Ober BA (2000) *California Verbal Learning Test* (Psychological Corp, San Antonio, TX), 2nd Ed.
- Meyers JE, Meyers KR (1995) *Rey Complex Figure Test and Recognition Trial* (Psychological Assessment Resources, Odessa, FL).
- Lezak MD, Howieson DB, and Loring DW (2004) *Neuropsychological Assessment*. (Oxford Univ Press, New York).
- Quiroga RQ, Nadasy Z, Ben-Shaul Y (2004) Unsupervised spike detection and sorting with wavelets and superparamagnetic clustering. *Neural Comput* 16(8):1661–1687.
- Pedreira C, et al. (2010) Responses of human medial temporal lobe neurons are modulated by stimulus repetition. *J Neurophysiol* 103(1):97–107.
- Rutishauser U, Mamelak AN, Schuman EM (2006) Single-trial learning of novel stimuli by individual neurons of the human hippocampus-amygdala complex. *Neuron* 49(6):805–813.
- Fried I, MacDonald KA, Wilson CL (1997) Single neuron activity in human hippocampus and amygdala during recognition of faces and objects. *Neuron* 18(5):753–765.
- Fried I, et al. (1999) Cerebral microdialysis combined with single-neuron and electroencephalographic recording in neurosurgical patients. Technical note. *J Neurosurg* 91(4):697–705.
- Gumprecht HK, Widenka DC, Lumenta CB (1999) BrainLab VectorVision Neuro-navigation System: Technology and clinical experiences in 131 cases. *Neurosurgery* 44(1):97–104.
- Schlaier JR, et al. (2004) Image fusion of MR images and real-time ultrasonography: Evaluation of fusion accuracy combining two commercial instruments, a neuro-navigation system and an ultrasound system. *Acta Neurochir (Wien)* 146(3):271–276, discussion 276–277.
- Teo PC, Sapiro G, Wandell BA (1997) Creating connected representations of cortical gray matter for functional MRI visualization. *IEEE Trans Med Imaging* 16(6):852–863.
- Amaral DG, Insausti R (1990) The hippocampal formation. *The Human Nervous System*, ed Paxinos G (Academic, San Diego), pp 711–755.
- Duvernoy HM, *The Human Hippocampus: Functional Anatomy, Vascularization, and Serial Sections with MRI* 1998 (Springer, Berlin).
- Ekstrom AD, et al. (2009) Advances in high-resolution imaging and computational unfolding of the human hippocampus. *Neuroimage* 47(1):42–49.
- Viskontas IV, Ekstrom AD, Wilson CL, Fried I (2007) Characterizing interneuron and pyramidal cells in the human medial temporal lobe in vivo using extracellular recordings. *Hippocampus* 17(1):49–57.
- Suthana N, Fried I (2012) Percepts to recollections: Insights from single neuron recordings in the human brain. *Trends Cogn Sci* 16(8):427–436.

Supporting Information

Suthana et al. 10.1073/pnas.1423036112

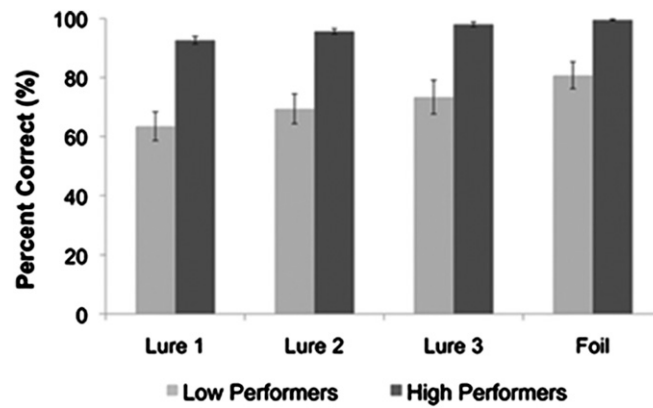


Fig. S1. Shown is percentage correct for the 40 sessions from 25 patients ($n = 40$) split into low and high performers. Lure 1 is the most similar and lure 3 is the least similar photograph to the target photograph, and the foil image is a novel photograph of an unstudied face.

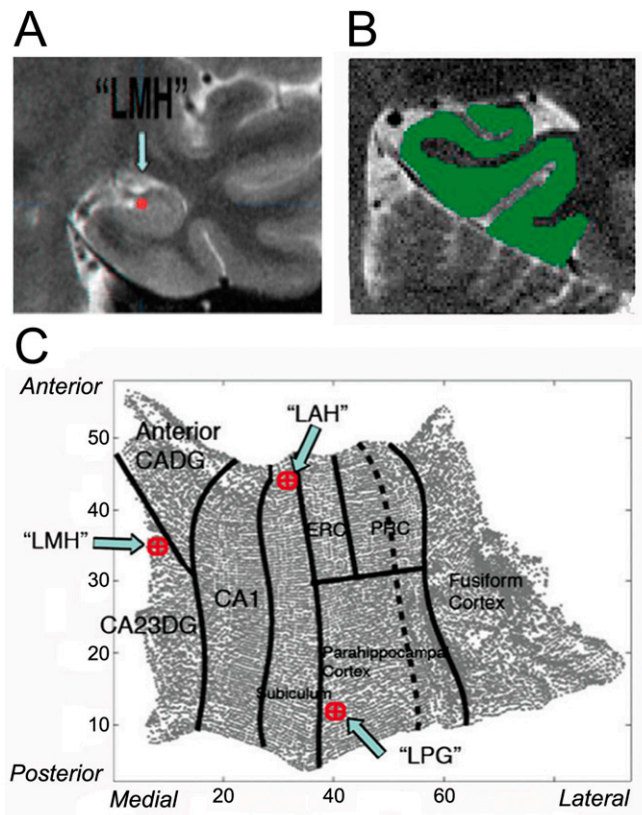


Fig. S2. (A) High-resolution MRI showing a left medial hippocampal (LMH) electrode location. (B) The 3D gray matter of the medial temporal lobe was created by manual segmentation of the gray matter on the high-resolution MRI. (C) An example patient's 2D flat map was created by unfolding the 3D gray matter and projecting electrode locations (shown in red). Regions shown are CA2, CA3, and dentate gyrus (CA23DG), anterior CA fields and dentate gyrus (CADG), CA1, subiculum, entorhinal cortex (ERC), parahippocampal cortex, perirhinal cortex (PRC), and fusiform cortex.

Table S1. Cont.

Patient	Placement	Localization	Patient	Placement	Localization
#11	LPG	LPHC		REC	REC
	RA	Amygdala		LEC	LEC
	LA	Amygdala		RPG	RPHC
	RAH	CA3DG		LPG	LPHC
	LAH	CA3DG		LA	Amygdala
	REC	REC			
	LEC	Subiculum			
	RPG	RPHC			
	LPG	LPHC			
	RA	Amygdala			
LA	Amygdala				

Region placements shown are right and left anterior, medial, or posterior hippocampus (RAH, LAH, RMH, LMH, RPH, LPH), right and left parahippocampal cortex (RPHC and LPHC), right and left entorhinal cortex (REC and LEC), and right and left amygdala (RA and LA). Electrodes from 22 of 25 subjects were further localized to the encompassing hippocampal subregions CA3 and dentate gyrus (CA3DG), CA1, or subiculum.

Table S2. Demographics and clinical characteristics of low and high performers

	Age	Sex	WAIS VIQ	WAIS digit span	WMS verbal memory	CVLT verbal memory	Rey-Osterrieth visual memory	Trails B executive
LP (mean)	31.75	7 (5)	90.1	27.17	18.17*	14.33*	9	29.2
SEM	3.23		4.27	9.05	4.16	5.96	7.67	10.08
HP (mean)	34.62	6 (5)	98.09	44.17	59.82*	53.82*	29.3	20.18
SEM	3.23		5.24	9.97	7.89	6.88	7.71	8.32

Shown are the average (bolded) and SE (SEM) of the ages and neuropsychological test scores in both groups. Under sex, is shown the number of male and female (in parentheses) participants within each group. Verbal IQ (VIQ) and digit span (attention) scores (percentiles shown) were calculated by using the Wechsler Adult Intelligence Scale (WAIS). Long-term verbal memory percentiles were calculated by using the Wechsler Memory Scale (WMS) and California Verbal Learning Test (CVLT) and executive function by means of the Trail Making Test. The asterisks (*) indicate significant differences between low performers (LP) and high performers (HP).

Table S3. Number of recorded units

Region	Multi-units	Single-units	Total units
Hippocampus	105	180	285
CA3DG	(62)	(117)	(179)
CA1	(9)	(7)	(16)
Subiculum	(34)	(56)	(90)
Entorhinal cortex	111	141	252
Parahippocampal cortex	88	138	226
Amygdala	176	237	413
Total	480	696	1,176

A total of 1,176 units were recorded from, with 285 in the hippocampus (179 in CA3 and dentate gyrus, 16 in CA1, and 90 in the subiculum), 252 in the entorhinal cortex, 226 in the parahippocampal cortex, and 413 in the amygdala. All performers ($n = 40$ sessions).

Table S4. Number of units in hippocampal CA3DG and subiculum regions, entorhinal cortex, parahippocampal cortex, and amygdala recorded from low performers

Region	Multi-units	Single-units	Total units
Hippocampus	47	82	129
CA3DG	(28)	(55)	(83)
CA1	(3)	(1)	(4)
Subiculum	(7)	(16)	(23)
Entorhinal cortex	50	83	133
Parahippocampal cortex	43	66	109
Amygdala	79	136	215
Total	204	343	586

Low performers ($n = 20$).

Table S5. Number of units in hippocampal CA3DG and subiculum regions, entorhinal cortex, parahippocampal cortex, and amygdala recorded from high performers

Region	Multi-units	Single-units	Total units
Hippocampus	58	98	156
CA3DG	(32)	(55)	(87)
CA1	(4)	(3)	(7)
Subiculum	(20)	(26)	(46)
Entorhinal cortex	61	58	119
Parahippocampal cortex	45	72	117
Amygdala	97	101	198
Total	251	298	590

High performers ($n = 20$).